Electronic supplementary information (ESI)

Post transition metal substituted Keggin POMs as thin film chemiresistive sensors for H_2O and CO_2 detection

Abigail A. Seddon,[a] Nathan S. Hill,[b] R. John Errington,[a] Pablo Docampo,[c] and Elizabeth A. Gibson*[a]

a. Energy Materials Laboratory, Chemistry, School of Natural and Environmental Sciences, Newcastle University, Newcastle upon Tyne, UK. Elizabeth.gibson@newcastle.ac.uk

b. School of Mathematics, Statistics, and Physics, Newcastle University, Newcastle upon Tyne, UK.

c. School of Chemistry, University of Glasgow, Glasgow, UK.

Experimental

All chemicals were purchased from Sigma Aldrich unless specified otherwise.

Synthesis of $Na_3[PW_{12}O_{40}].8H_2O$

$H_3PW_{12}O_{40}.xH_2O$ (50.30 g, 17.46 mmol) was added to distilled H_2O (20 mL) whilst stirring. Excess NaCl (9.26 g, 0.158 mol) was added instantly forming a white precipitate. The solution was washed, filtered, and dried via a Buchner filter and then vacuum-dried overnight. ^{31}P NMR (300 MHz, CD_3CN): δ = -15.22 ppm.

Synthesis of $(TBA)_6[NaPW_{11}O_{39}]$

$Na_3[PW_{12}O_{40}].8H_2O$ (5.55 g, 1.80 mmol) was dissolved in MeCN (Acros Organics from Fisher Scientific, 15 mL) and cooled to -30 °C. 1 M methanolic TBA(OH) (10.0 mL, 10.0 mmol) was added slowly with continuous stirring. The resulting solution was left to settle for around 4 hours, filtered via a cannula filter stick using 0.22 µm pore size filter paper and vacuum dried to give a cream-coloured gel. The gel was triturated with diethyl ether (Acros Organics from Fisher Scientific, ~40 mL x 4) and vacuum dried again to obtain a white powder. The white solid was re-dissolved by gentle heating in MeCN (5 mL) to give a clear

solution with some precipitate, which was left to settle overnight before filtering the following day. The clean filtrate was vacuum dried and stored under argon. ^{31}P NMR (300 MHz, CD_3CN): δ = -10.62 ppm.

Synthesis of $(TBA)_4[BiPW_{11}O_{39}]$

$(TBA)_6[NaPW_{11}O_{39}]$ (2.07 g, 0.49 mmol) was dissolved in MeCN (10 mL) whilst stirring. $BiCl_3$ (0.157 g, 0.49 mmol) was added, forming a cloudy solution which was stirred for 1 h and allowed to settle overnight. The top clear solution was filtered via cannula filter stick, vacuum-dried and washed with EtOAc (10 mL x 3) before vacuum-drying again to obtain a white solid. ^{31}P NMR (300 MHz, CD_3CN): δ = -12.27 ppm.

Synthesis of $(TBA)_5[PbPW_{11}O_{39}]$

$(TBA)_6[NaPW_{11}O_{39}]$ (1.15 g, 0.28 mmol) was dissolved in MeCN (5 mL). $Pb(CH_3COO)_2.3H_2O$ (0.107 g, 0.28 mmol) was added whilst stirring, forming a white precipitate. The solution was stirred for 1 h before allowing it to settle overnight. The top clear solution was filtered via cannula filter stick and vacuum dried. The white solid obtained was triturated with EtOAc (10 mL x 3) and diethyl ether (10 mL) before drying under vacuum. ^{31}P NMR (300 MHz, CD_3CN): δ = -11.98 ppm.

Synthesis of $(TBA)_4[SbPW_{11}O_{39}]$

$(TBA)_6[NaPW_{11}O_{39}]$ (3.67 g, 0.88 mmol) was dissolved in MeCN (36.7 mL). $SbCl_3$ (0.20 g, 0.88 mmol) was added, forming a white precipitate. The solution was stirred for 1 h and canulated into centrifuge tubes and spun for (4200 rpm) for 15 minutes. The supernatant was collected and vacuum-dried, washed with DCM (10 mL x 3) and vacuum-dried to obtain a white solid. ^{31}P NMR (300 MHz, CD_3CN): δ = -14.21 ppm.

Electrode Preparation

5 layers of a 10 mg mL^{-1} POM in MeCN solution was applied onto a cleaned laser-etched (ULYXE DPSS laser etcher) indium tin oxide (ITO, Sigma Aldrich) coated glass electrode (Figure S1) using a doctor blade technique, using a Scotch tape (3M) mask. The cleaning procedure was as follows: immersion of the conductive glass slides for 10 minutes each in a sonic bath with Decon®90 soap (Decon® laboratories) + deionised water (DI), DI water only, acetone, and ethanol, followed by ozone cleaning (NOVASCAN PSD-UV). ITO substrates were 20 mm x 20 mm in size. Finally, a 4 mm strip of POM was removed from each side with ethanol and conductive silver paste (Sigma Aldrich) was applied to improve

the connection between the ITO and metal pins. Polyaniline (PANI) films were deposited by spin coating a PANI solution at 500 rpm for 30 s followed by 3000 rpm for 5 s. 20 mg/mL of PANI (Emeraldine Salt, Merck Life Sciences) in N,N-dimethylformamide (Merck Life Sciences) was prepared, sonicated for ~30 hours, and filtered prior to deposition. Polymethylmethacrylate (PMMA) films were prepared by spin coating 100 mg/mL PMMA in chlorobenzene (Merck Life Sciences) at 1000 rpm for 45 s.

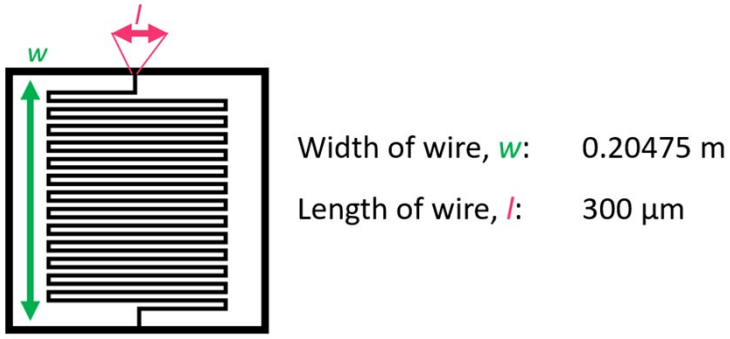

Figure S1. Diagram of ITO interdigitated electrodes with 'width' and 'length' of the channel (wire).

Two-point Probe for Humidity Testing

Current-voltage (IV) measurements were performed between -2 V and 2 V with a step size of 0.1 V and scan rate of 1 Vs^{-1}. Measurements were taken in the forward and reverse direction. The resistance of the device was calculated through the inverse slope of the resultant linear plot, from which the conductivity was calculated using equation 1.[1] The length and width of the channel were measured with an optical microscope.

$$R = \frac{V}{I} = \rho\left(\frac{L}{A}\right); \qquad \sigma = \frac{1}{\rho}; \qquad (1)$$

Where σ: conductivity, ρ: resistivity, R: resistance in ohms, L: length in metres, A: the area in m^2, V: voltage, and I: current.

Samples were measured in a humidity-controlled environment with a purpose-built holder and printed circuit board (PCB), coupled with a QTenki humidity sensor and temperature probe (Dracal Technologies). The appropriate gas (either air, N_2, or CO_2 only) was passed through the water bubbler before passing through the sample container. The container was

purged for 15 minutes with the respective gas prior to each measurement. The flow rate was adjusted to control the humidity. Four repeat measurements were taken for each POM electrode.

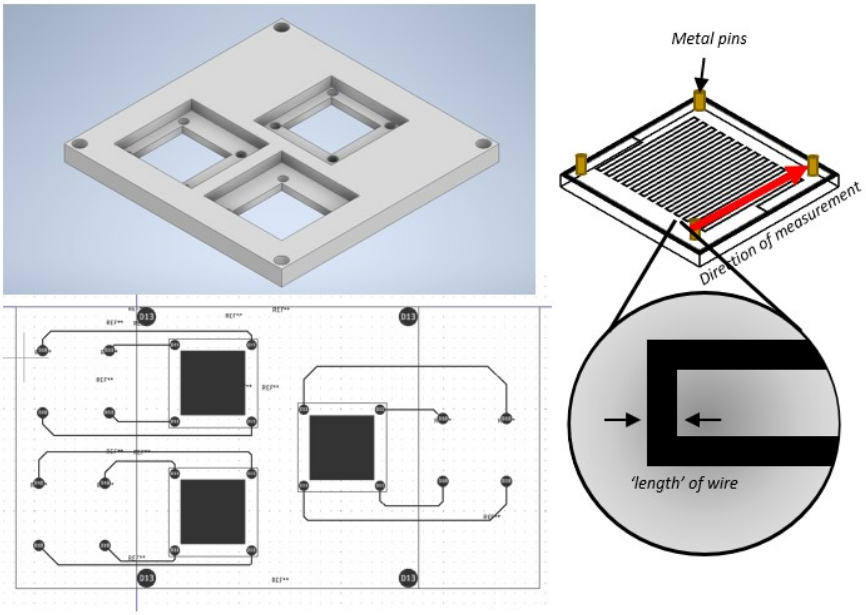

Figure S2. Experimental set-up for conductivity measurements. Top left: design for sample holder, bottom left: design for PCB, right: electrode pattern and contacts.

The sensitivity of these measurements can be improved by increasing the area of the wire, which is achieved by creating an etched channel on the ITO substrate in a finger pattern (Figure S1). If the area of the wire is increased, a larger current can be read by the source meter.

Four-point Probe for Electrode Sheet Resistance

Circular (1 cm diameter) electrodes were fabricated by doctor blading 10 mg mL^{-1} solutions of POM in MeCN onto ITO and measured on an Ossila four-point probe setup. Measurement parameters were as follows: 2048 samples per point, probe spacing of 1.27 mm, target current 100 mA, maximum voltage 10 V, voltage increment 0.010 V, and 25 repeats of each electrode. The resistivity of the material was measured in accordance with the following equation:

$$R_s = \frac{\pi \ \Delta V}{\ln 2 \ I} \qquad (2)$$

Where R_s: sheet resistance, ΔV: difference in voltage measured between the inner probes, I: current applied to outer probes.

AFM

A Digital Instruments Multimode-8 with a NanoScope V controller and E scanners (Bruker) was used for acquiring AFM images. The AFM data were analysed with NanoScope Analysis 1.50 software (Bruker). The AFM was operated in tapping mode. An isolation table (Veeco Inc., Metrology Group) was used to minimise vibrational noise. Aluminium-coated silicon tips on silicon cantilevers (Tap300Al-G, BudgetSensors) were used for imaging. The nominal tip curvature radius was approximately <10 nm, resonant frequency ~300 kHz and spring constant k ~ 40 N m^{-1}. The film thickness was measured by using the AFM tip at a strong force in contact mode to scratch away a 1 μm^2 area of the of the film (aspect ratio 20:1), exposing the glass underneath. A new tip was then used to image the area in tapping mode over the scratch to measure the height in the z-direction of the film.

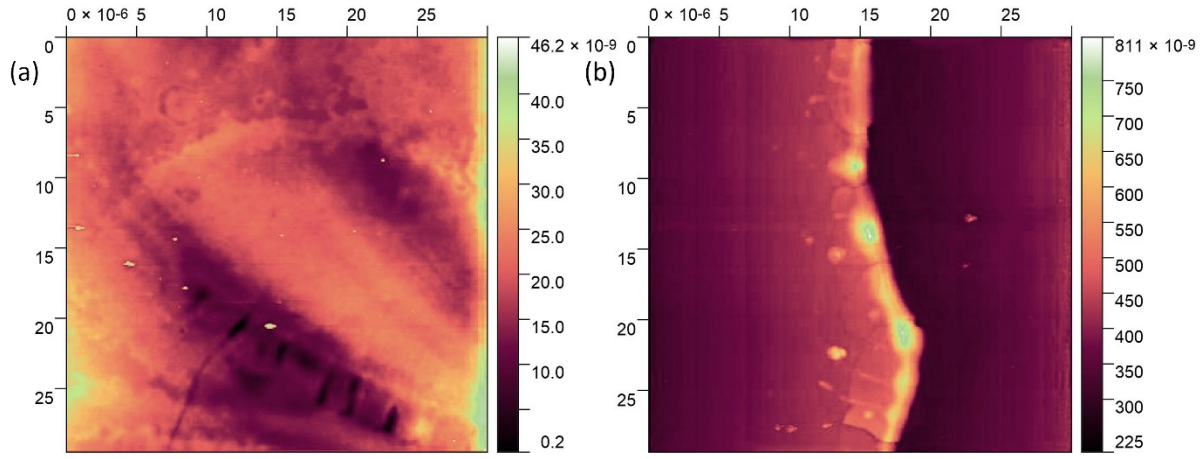

Figure S3. AFM images of a film of PMMA deposited onto an interdigitated ITO electrode. (a) shows the surface of the electrode which consists of PMMA on bare glass, (b) shows the edge of the electrode/ITO interface. Colour bars show z-axis height of the surface (nm), whilst x- and y- axes show area analysed (nm).

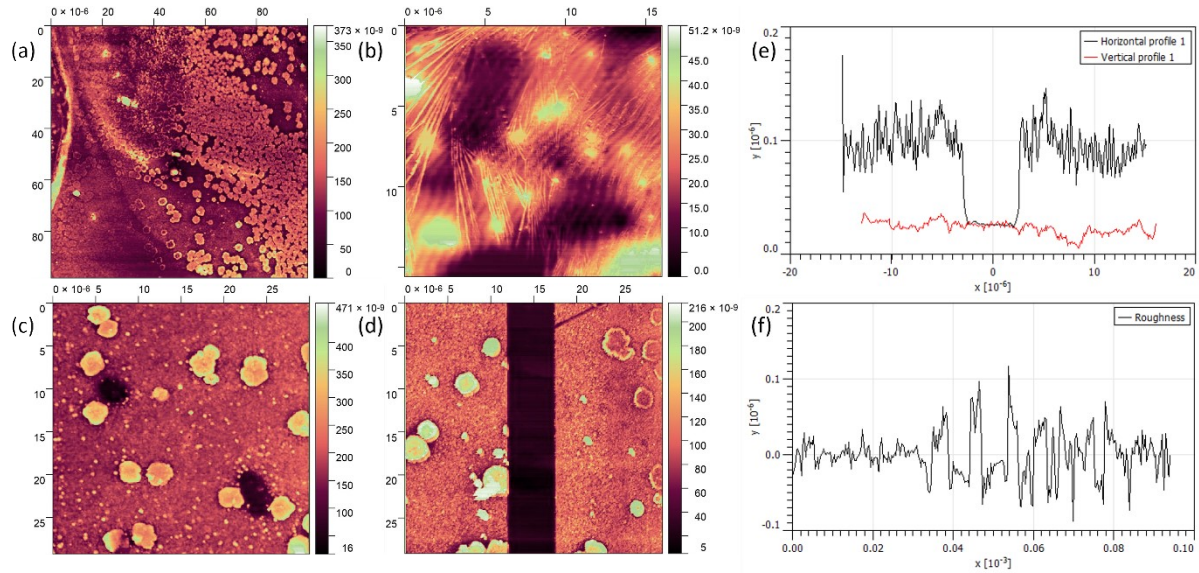

Figure S4. AFM images of a film of $(TBA)_6[NaPW_{11}O_{39}]$ deposited onto an interdigitated ITO electrode. (a) shows the surface of the electrode, (b) shows the POM on the ITO surface, (c) shows POM clusters on the electrode surface, (d) scratch used for thickness measurements, (e) profile of the scratch in (d) to obtain film thickness, and (e) shows the roughness of the electrode surface of (c). Colour bars show z-axis height of the surface (nm), whilst x- and y-axes show area analysed (µm) for (a-d). In (e-f), y-axis shows height (µm) and x-axis shows distance in the x-direction (nm).

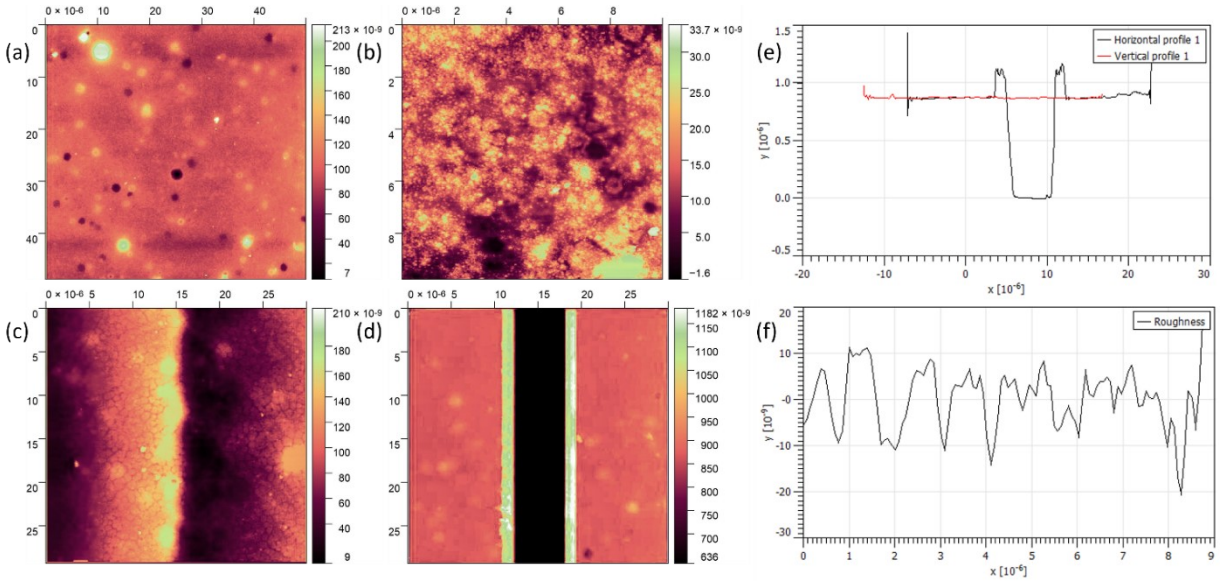

Figure S5. AFM images of a film of $(TBA)_5[PbPW_{11}O_{39}]$ deposited onto an interdigitated ITO electrode. (a) shows the surface of the electrode, (b) electrode surface at a higher magnification, (c) shows the electrode edge with observable POM clusters, (d) scratch used for thickness measurements, (e) profile of the scratch in (d) to obtain film thickness, and (e)

shows the roughness of the electrode surface of (a). Colour bars show z-axis height of the surface (nm), whilst x- and y-axes show area analysed (µm) for (a-d). In (e-f), y-axis shows height (µm) and x-axis shows distance in the x-direction (µm).

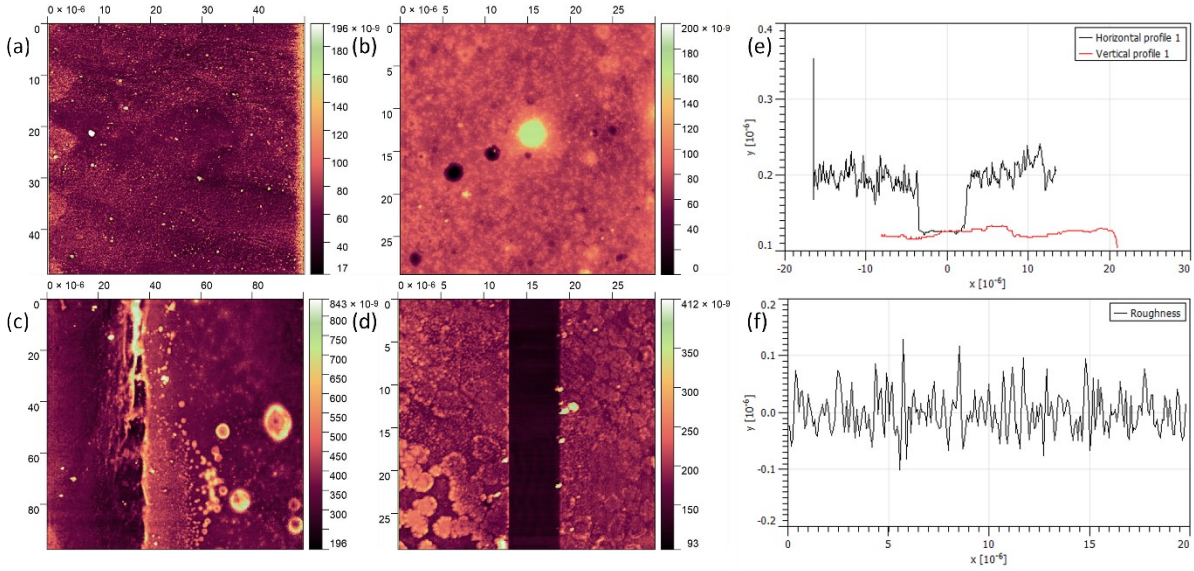

Figure S6. AFM images of a film of $(TBA)_4[SbPW_{11}O_{39}]$ deposited onto an interdigitated ITO electrode. (a) shows the surface of the electrode, (b) electrode surface at a higher magnification, (c) shows the electrode edge with observable POM clusters, (d) scratch used for thickness measurements, (e) profile of the scratch in (d) to obtain film thickness, and (e) shows the roughness of the electrode surface of (b). Colour bars show z-axis height of the surface (nm), whilst x- and y-axes show area analysed (nm) for (a-d). In (e-f), y-axis shows height (µm) and x-axis shows distance in the x-direction (µm).

Table S1. Film thickness, average roughness (Ra), and root mean square roughness (Rq) from AFM measurements of POM thin films. Analysed with Gwyddion version 2.63.

POM	Film thickness (nm)	R_a roughness (nm)	R_q roughness (nm)
$(TBA)_6[NaPW_{11}O_{39}]$	147.7 ± 15.1	21.51 ± 1.28	29.47 ± 1.34
$(TBA)_4[BiPW_{11}O_{39}]$	54.5 ± 3.3	2.50 ± 0.04	3.07 ± 0.05
$(TBA)_5[PbPW_{11}O_{39}]$	878.4 ± 4.9	5.22 ± 0.06	6.48 ± 0.07
$(TBA)_4[SbPW_{11}O_{39}]$	64.5 ± 2.3	7.99 ± 0.05	6.14 ± 0.06

Conductivity

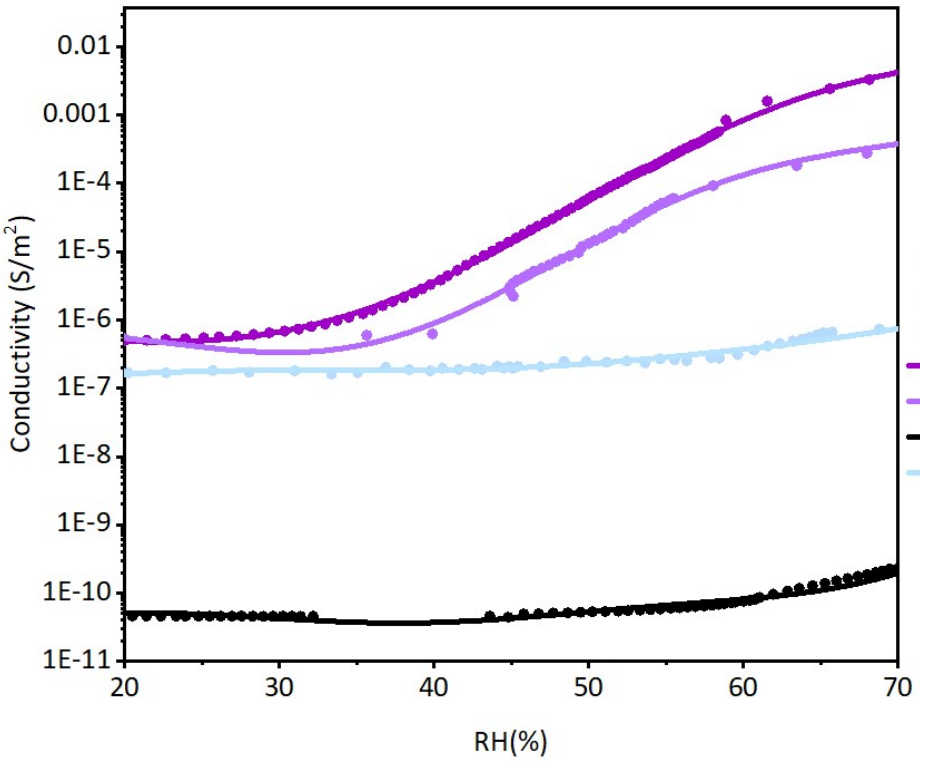

Figure S7. Conductivity vs. relative humidity (%) of glass (black) and films of 'thin' polyaniline (lilac), 'thick' polyaniline (purple), PMMA (blue).

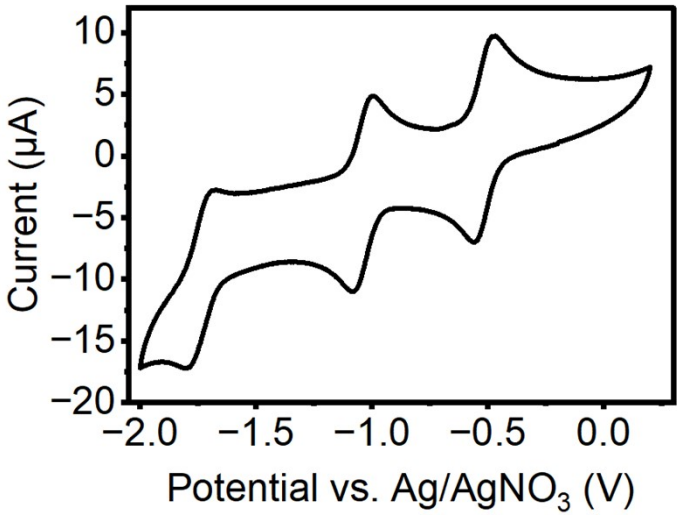

Figure S8. Cyclic voltammogram of $TBA_3PW_{12}O_{40}$ recorded as 0.2 mM POM, and 0.2 M $TBAPF_6$ in dry MeCN. Glassy carbon W.E., Pt wire C.E., and $Ag/AgNO_3$ reference electrode. The solution was bubbled with argon for 15 minutes prior to measurement. Current is plotted against the square root of scan rate to establish reversibility. From darkest to

lightest, scan rate at 100 mV s^{-1}. On the right, solid lines show reduction and dashed lines show oxidation as labelled.

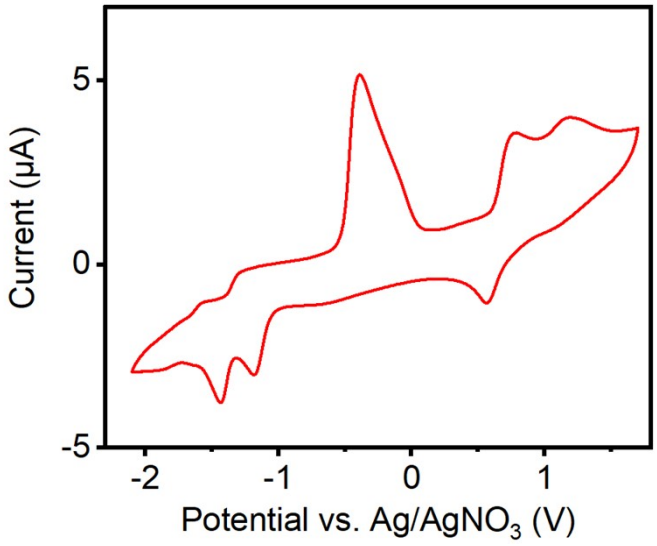

Figure S9. Cyclic voltammogram of $(TBA)_4[BiPW_{11}O_{39}]$ recorded as 0.2 mM POM, and 0.2 M $TBAPF_6$ in dry MeCN. Glassy carbon W.E., Pt wire C.E., and $Ag/AgNO_3$ reference electrode. The solution was bubbled with argon for 15 minutes prior to measurement. Current is plotted against the square root of scan rate to establish reversibility. From darkest to lightest, scan rate at 100 mV s^{-1}. On the right, solid lines show reduction and dashed lines show oxidation as labelled.

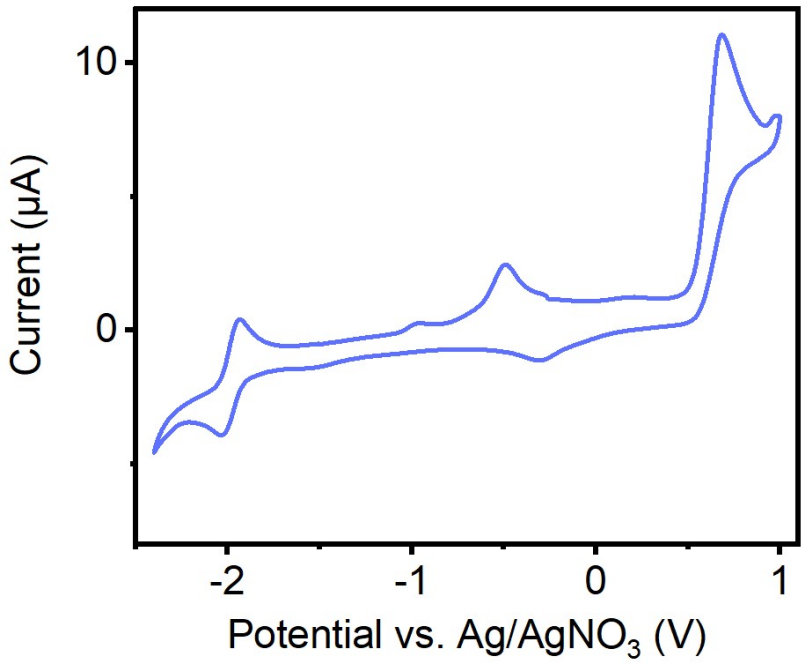

Figure S10. Cyclic voltammogram of $(TBA)_5[PbPW_{11}O_{39}]$ recorded as 0.2 mM POM, and 0.2 M $TBAPF_6$ in dry MeCN. Glassy carbon W.E., Pt wire C.E., and $Ag/AgNO_3$ reference electrode. The solution was bubbled with argon for 15 minutes prior to measurement. Current is plotted against the square root of scan rate to establish reversibility. From darkest to lightest, scan rate at 100 mV s^{-1}. On the right, solid lines show reduction and dashed lines show oxidation as labelled.

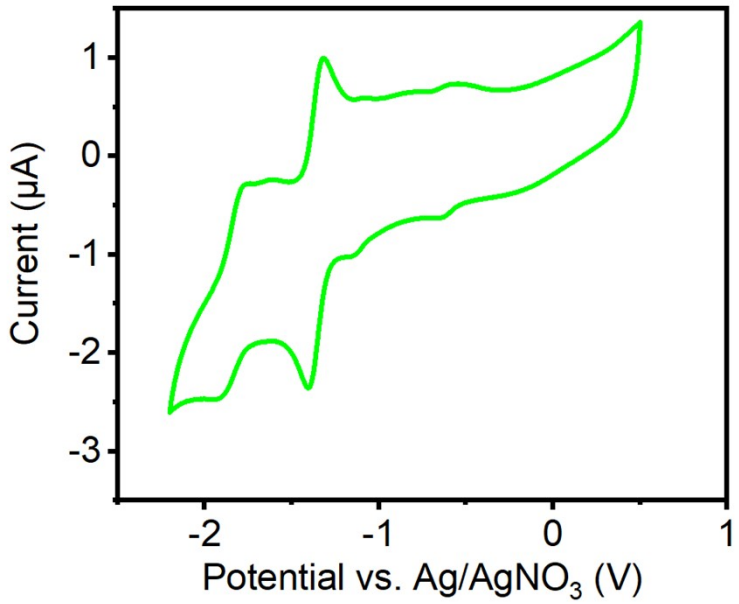

Figure S11. Cyclic voltammogram of $(TBA)_4[SbPW_{11}O_{39}]$ recorded as 0.2 mM POM, and 0.2 M $TBAPF_6$ in dry MeCN. Glassy carbon W.E., Pt wire C.E., and $Ag/AgNO_3$ reference electrode. The solution was bubbled with argon for 15 minutes prior to measurement. Current is plotted against the square root of scan rate to establish reversibility. From darkest to lightest, scan rate at 100 mV s^{-1}. On the right, solid lines show reduction and dashed lines show oxidation as labelled.

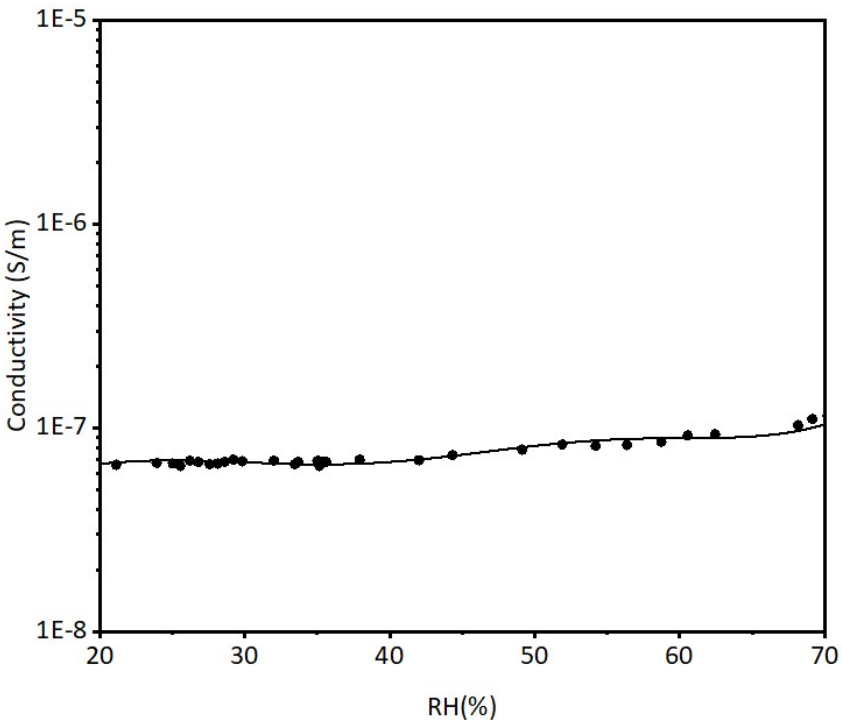

Figure S12. Conductivity vs. relative humidity (%) for a thin film of $TBA_3PW_{12}O_{40}$.

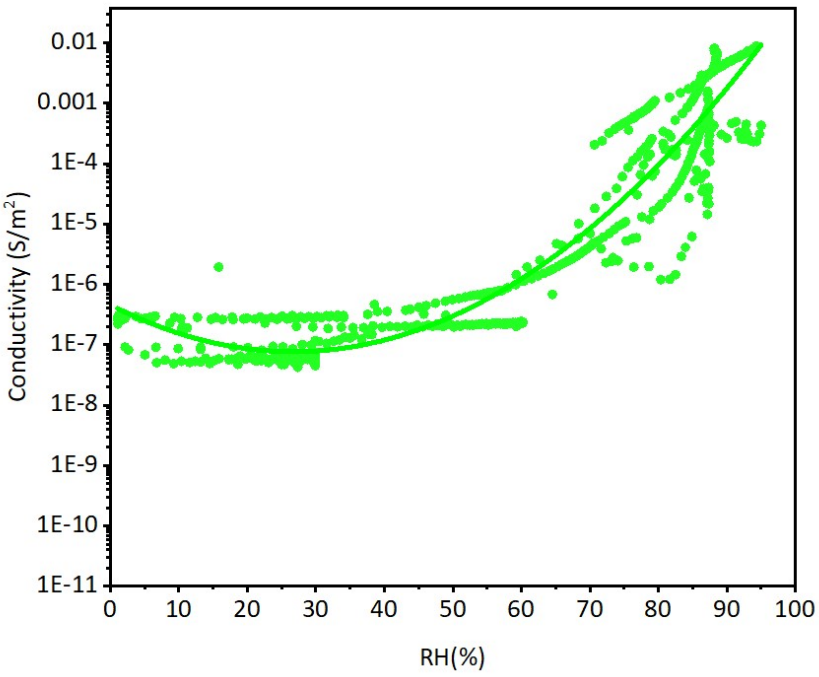

Figure S13. Conductivity vs. relative humidity (%) for a thin film of $(TBA)_4[BiPW_{11}O_{39}]$ after repeated exposure to H_2O and CO_2, indicating reusability.

References

1 R. J. Errington, Advances in Inorganic Chemistry, 2017, 69, 287-336

2 T. Izuagie, PhD Thesis, Newcastle University, 2017

3 R. J. Errington in Comprehensive Coordination Chemistry II, Vol. 2, Elsevier: Amsterdam, 2003; pp 759–773

4 R. J. Errington in Polyoxometalate Molecular Science; J. J. Borrás-Almenar, E. Coronado, A. Müller, M. T. Pope Eds.; Kluwer: Dordrecht, 2003; pp 55–77

5 R. J. Errington in Polyoxometalate Chemistry: From Topology via Self-Assembly to Applications; M. T. Pope, A. Muller Eds.; Kluwer: Dordrecht, 2001; pp 1–22

6 G. Ohm, Die galvanische Kette, mathematisch bearbeitet, Bei T. H. Riemann., Berlin, 1827

7 A. Seddon, PhD Thesis, Newcastle University, 2023